Corrosion Science 77 (2013) 397–402

Contents lists available at ScienceDirect

Corrosion Science

journal homepage: www.elsevier.com/locate/corsci

Short Communication

# Investigation into the high temperature oxidation of Cu-bearing austenitic stainless steel using simultaneous electron backscatter diffraction-energy dispersive spectroscopy analysis

Ju-Heon Kim [a,b], Dong-Ik Kim [a,*], Jae-Hyeok Shim [a], Kyung-Woo Yi [b]

[a] High Temperature Energy Materials Research Center, Korea Institute of Science and Technology, Hwarangno 14-gil 5, Seongbuk-gu, Seoul 136-791, Republic of Korea
[b] Department of Materials Science and Engineering, Seoul National University, 1 Gwanak-ro, Gwanak-gu, Seoul 151-744, Republic of Korea

ARTICLE INFO

*Article history:*
Received 23 May 2013
Accepted 20 August 2013
Available online 28 August 2013

*Keywords:*
A. Stainless steel
B. SEM
C. Oxidation

ABSTRACT

The oxide scales of high-alloyed steel are composed of complex phases that are difficult to differentiate with conventional analysis techniques. Here, we used simultaneous electron backscatter diffraction (EBSD) and energy dispersive X-ray spectroscopy (EDS) to analyze the complex oxide layers formed on a Cu-bearing austenitic stainless steel. Multi-layered structures of external hematite, external magnetite, internal chromite, internal chromium oxide, and austenite matrix were clearly identified using the simultaneous EBSD–EDS analysis technique. The addition of Cu into the austenitic stainless steel induced spinel structured oxide formation at the top surface of the external oxide.



## 1. Introduction

Over the past several decades, oxide layers formed on heat-resistant steels at high temperatures have been intensively investigated because they can lead to localized cracks and defects [1–4]. Generally, oxide layers formed during high-temperature oxidation consist of complex and discrete oxides with a variety of microstructures [5,6]. The addition of alloying elements imparts better heat resistance to steel but complicates this material's oxidation because the oxide phases are strongly dependent on the steel composition [7]. Conventional analysis techniques, such as X-ray diffraction and transmission electron microscopy, are widely used for complex oxide phase analysis. Recently, techniques based on scanning electron microscopy (SEM), such as energy dispersive X-ray spectroscopy (EDS), electron probe microanalysis, and electron backscatter diffraction (EBSD) have improved the analysis of oxide phases by providing statistically reliable phase and microstructural information [5,8,9]. Among these techniques, EBSD has the highest spatial resolution (several tens of nanometers). EBSD differentiates phases while providing crystallographic orientation; however, EBSD is limited in terms of phase discrimination in cases in which the candidate phases have similar crystallographic structures [10,11]. The accuracy of phase discrimination can be enhanced by virtue of chemical information collected by EDS [12–14]. Over the last decade, the EDS measurement speed has increased dramatically due to the development of silicon drift detector technology, large EDS detectors and improved signal processing unit technology. The speed of EDS data acquisition is now comparable with that of EBSD and a simultaneous real-time EBSD–EDS analysis technique is applicable for distinguishing complex oxide layers consisting of multiple phases with similar crystal structures.

Cu is one of the alloying elements considered for the strengthening of heat resistant steels [15,16]. While the effects of Cu addition on the mechanical properties of steels have been investigated previously [17–19], only a limited number of reports are available regarding the effects on the high temperature oxidation behavior of steels [20,21]. In the present study, we investigated the oxide scale formed on Cu-bearing 304H grade austenitic stainless steels using the simultaneous EBSD–EDS analysis technique. A multi-layered complex oxide structure with hematite ($Fe_2O_3$), magnetite ($Fe_3O_4$), chromite ($FeCr_2O_4$), chromium oxide ($Cr_2O_3$), and Cu-containing spinel ($Fe_2CuO_4$) was observed in the internal and external oxide regions. The effect of Cu addition on the composition of the oxide layer is discussed based on the compositional and microstructural analysis of the oxide.

## 2. Experimental

The material used in this study was a Cu-bearing austenitic stainless steel. The chemical composition of investigated steel is tabulated in Table 1. It was fabricated by vacuum induction melting in laboratory scale (6.5 kg ingot). The ingot was homogenized at 1200 °C for 24 h and then forged to a thickness of 30 mm at the same temperature. Samples for the oxidation test were cut from the forged specimen and annealed at 1200 °C for 30 min to

* Corresponding author. Tel.: +82 2 958 5432; fax: +82 2 958 5379.
*E-mail addresses:* dongikkim@kist.re.kr, dongikkim@gmail.com (D.-I. Kim).

0010-938X/$ - see front matter © 2013 Elsevier Ltd. All rights reserved.
http://dx.doi.org/10.1016/j.corsci.2013.08.015

**Table 1**
Chemical composition of Cu-bearing austenitic stainless steel (in wt.%).

| Fe | Cr | Ni | Mn | Cu | Nb | Si | C | N |
|---|---|---|---|---|---|---|---|---|
| Bal. | 18.06 | 9.25 | 0.755 | 2.96 | 0.38 | 0.198 | 0.112 | 0.1621 |

remove a deformed microstructure generated during forging process. Oxidation tests were performed on 10 × 7 × 1.2 mm samples at 700 °C in tube furnace under the 20% humidity containing air condition for 500 h. After oxidation and Au deposition, the samples were coated in epoxy resin to protect the brittle oxide scale. For cross-sectional analysis, the edges of the sample were ground on 2000-grit silicon carbide paper and ion-milled at 6 kV for 5 h using a cross-sectional ion miller (E-3500, Hitachi, Japan). Simultaneous EBSD–EDS analysis was performed using the CrystAlign system with an EBSD (*e*-Flash$^{HR}$, Bruker, Germany) and an EDS (XFlash, Bruker, Germany) mounted on a field emission gun SEM (S-4300SE, Hitachi, Japan). The EBSD/EDS maps were processed using Esprit software (version 1.9.4). For the detailed procedure for simultaneous EBSD–EDS analysis will be given in the results and discussion session.

An EBSD/EDS map consisting of 132,000 points covering an area of 81.92 × 30.17 μm was acquired at a 20 kV acceleration voltage with a 4 nA probe current. A fine step size (0.14 μm) was used to observe the fine grains of the oxide layer. Each EBSD–EDS dataset was acquired for 51 ms with three frames of integration averaging to produce high-quality EBSD patterns with a sufficient number of counts in each EDS spectrum (~3000). All datasets and figures are presented in their original state without data cleaning.

## 3. Results and discussion

The oxidized Cu-bearing austenitic stainless steel is composed of seven phases: austenite matrix (γ-Fe), ferrite (α-Fe), chromium oxide ($Cr_2O_3$), hematite ($Fe_2O_3$), magnetite ($Fe_3O_4$), chromite ($FeCr_2O_4$) [22], and Cu-containing spinel ($Fe_2CuO_4$). Fig. 1 presents the crystal structures and simulated Kikuchi patterns of these phases. These phases have different space groups, as follows: austenite: Fm-3m, ferrite: Im-3m, chromium oxide: R-3c, hematite: R-3c, magnetite: Fd-3m, chromite: Fd-3m, and Cu-containing spinel: Fd-3m. The EBSD patterns for the three spinel structure phases and the two rhombohedral structure phases are the same. These EBSD patterns were similar to austenite, particularly for the high-intensity diffraction bands because the iron atoms from the austenite matrix have the same symmetry as the spinel oxide. The similarities among the EBSD patterns are problematic for identification of the oxide phases. Previous studies have shown that oxide analysis is possible using only EBSD, but these studies were limited to the oxidation of ferritic steels [5,23–26] or classified the phases with similar crystal structures to one category [27]. A combined analysis using EBSD and EDS improves phase identification [28,29]; however, it is difficult to implement combined analysis techniques because the complex oxides formed from multiple elements in alloyed steel require several steps of subset creation.

Fig. 2 presents the cross-section of the oxide from austenitic stainless steel oxidized at 700 °C for 100 h. Typically, the interface between the oxide and the matrix is easily observed with the secondary electron image (Fig. 2a). The pattern quality map (Fig. 2b) indicates that there is a transition layer of small oxides with low pattern quality at the oxide–matrix interface. This transition region is not indexed properly with EBSD, as shown in the phase

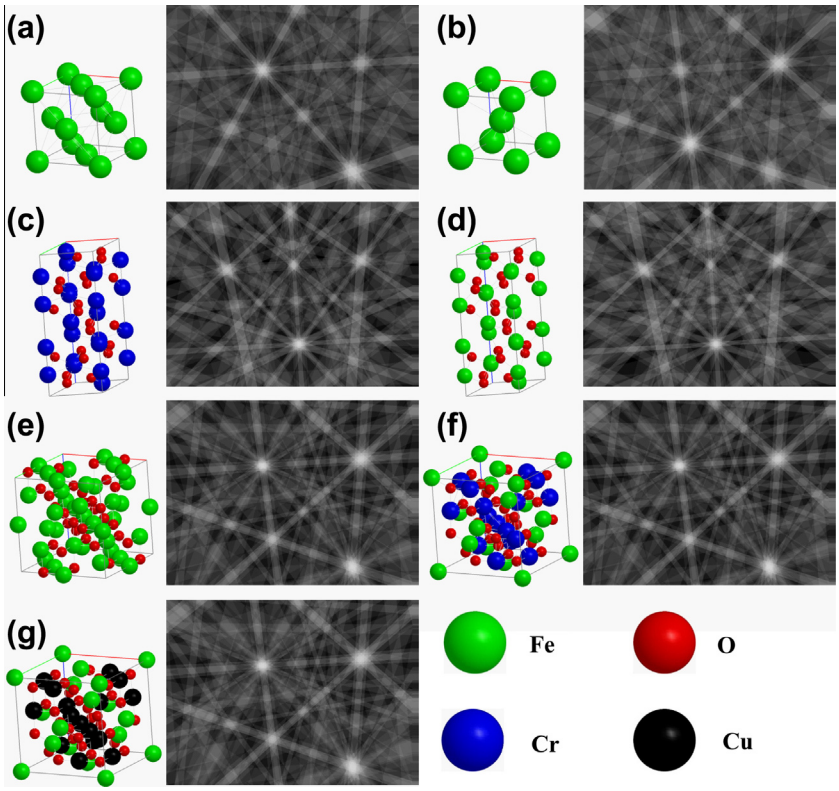


**Fig. 1.** Unit cells and corresponding spherical Kikichi patterns (kinematic simulation) of seven phases formed by oxidation heat treatment at 700 °C under the 20% humidity containing air condition in Cu bearing austenitic stainless steel: (a) austenite (γ-Fe), (b) ferrite (α-Fe), (c) chromium oxide ($Cr_2O_3$), (d) hematite ($Fe_2O_3$), (e) magnetite ($Fe_3O_4$), (f) chromite ($FeCr_2O_4$), and (g) Cu containing spinel ($Fe_2CuO_4$) at [Phi1, Phi, Phi2] = (30; −10; 0).